

Studies on MCM-41: Effect of sulfate on nitration of phenol

K.M. Parida*, Dharitri Rath

C & MC Cell, Regional Research Laboratory (CSIR), Bhubaneswar 751013, Orissa, India

Received 9 June 2006; received in revised form 14 July 2006; accepted 17 July 2006

Available online 30 August 2006

Abstract

The mesoporous molecular sieve MCM-41 was synthesized by sol–gel method using tetraethyl orthosilicate (TEOS), cetyl trimethyl ammonium bromide (CTAB), aqueous NH_3 and water. A series of sulfate modified MCM-41 was prepared by incipient wetness impregnation method using H_2SO_4 as sulfating agent. The samples were characterized by BET surface area, X-ray diffraction, FT-IR and TG–DTA. The catalytic activity of the samples was evaluated for nitration of phenol with nitric acid in dichloro ethane (DCE) medium, at room temperature. The effect of reaction parameters, i.e. time, concentration of nitric acid and phenol/nitric acid ratio were also investigated. Modification with sulfate opened new opportunities to generate active Brønsted and Lewis acid sites in the stabilized nanostructure MCM-41. Among the catalysts screened, 4 wt.% sulfated MCM-41 showed maximum activity (93%), with 90% selectivity towards *ortho*-nitrophenol.

© 2006 Elsevier B.V. All rights reserved.

Keywords: MCM-41; Sulfated MCM-41; Nitration; *ortho*-Nitrophenol

1. Introduction

Mesoporous molecular sieves designated as M41S have attracted the attention of many researchers since their discovery at Mobile Oil Corporation in 1992 [1]. These materials possess well-defined mesopores the diameters of which can be tailored to the desired value (18–100 Å) by the proper choice of surfactants, auxiliary organics and synthesis parameter [2]. Mesoporous silica of the MCM-41 type is an important class of a hexagonal arrangement of cylindrical pores between which an amorphous SiO_2 network is interposed [3,4]. The most interesting feature of MCM-41 is its regular pore system, which consists of a hexagonal array of one-dimensional, hexagonally shaped pores. Other interesting physical properties of MCM-41 include a highly specific surface area up to $1500 \text{ m}^2/\text{g}$, a specific pore volume up to 1.3 ml/g and a high thermal stability. All the above properties make it suitable for many catalytic applications.

Molecular sieves are widely used in acid catalyzed reactions for the production of petrochemicals and fine chemicals. The activity of these materials is attributed to their acidic character wherein Brønsted and Lewis acid sites are involved. The incor-

poration of acidity in clays, ion-exchange resins, metal oxides and zeolites has attracted considerable attention [5].

Modified MCM-41 has opened new opportunities in order to obtain new acid materials for catalytic applications. Some properties of a thermo stable mesophase of basic zirconium sulfate with textural characteristics close to those of MCM-41 have been reported [6]. The peculiarities of the catalytic behavior of the mesophase are related to its acidic properties. The MCM-41 nanostructured materials present ordered crystallographic channels and disordered atomic arrangement, similar to that of amorphous silica. The discovery offers the opportunity to extend shape selective catalysis beyond the micro pore domain typical of zeolite, allowing larger molecules to be transformed with large potential applications in the fine chemical industries. However studies showed that the thermal stability of MCM-41 is a function of textural properties that strongly depends upon the synthesis condition, such as the chemical composition, template applied and post treatment [7,8]. MCM-41 exhibits mild acidity, which is weaker than that of the micro porous zeolites [9]. The acidity of MCM-41 desired to be increased by incorporation of sulfate ions into the molecular sieves. The sulfated MCM-41 is used as an efficient catalyst for many acid catalyzed reactions. In this work the synthesis of sulfated MCM-41 was studied using the controlled impregnation method.

Nitration of aromatic substrates is a widely studied reaction of great industrial significance as many nitro aromatics are exten-

* Corresponding author. Tel.: +91 674 2581636x425; fax: +91 674 2581637.
E-mail address: kmparida@yahoo.com (K.M. Parida).

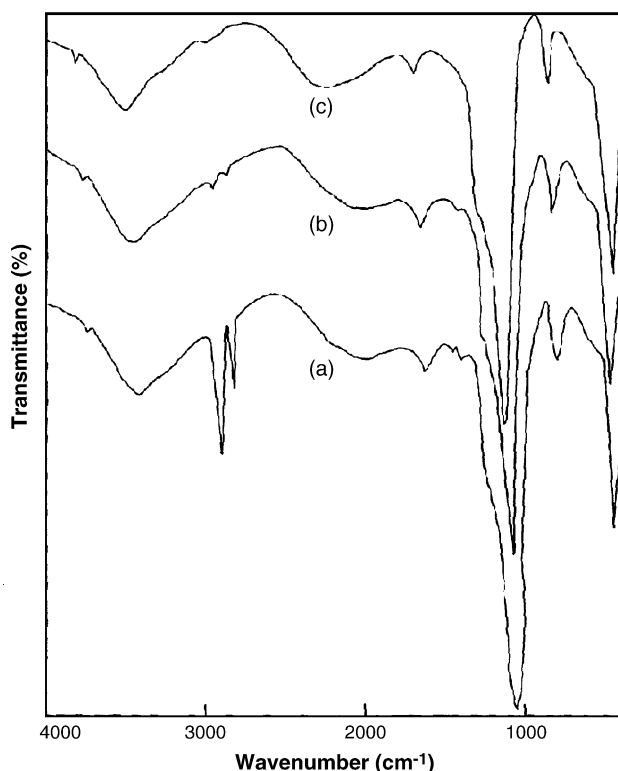
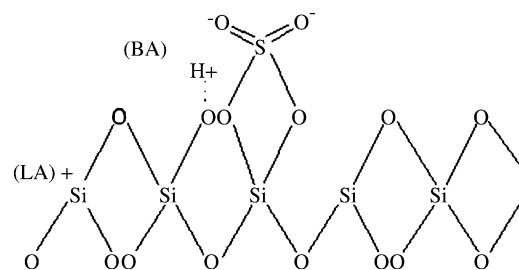


Fig. 2. FT-IR spectra of uncalcined MCM-41 (a), calcined MCM-41 (b) and sulfated MCM-41 (c).

The FT-IR spectra of MCM-41 and sulfated MCM-41 are shown in Fig. 2. The spectra showed a broad band around $3100\text{--}3600\text{ cm}^{-1}$, which is due to adsorbed water molecules. The absorption band due to H–O–H bending vibration in water is at $1620\text{--}1640\text{ cm}^{-1}$. The absorption band around $1087\text{--}1092\text{ cm}^{-1}$ is due to Si–O asymmetric stretching vibrations of Si–O–Si bridges. The absorption band at 964 cm^{-1} is due to Si–OH group that vanished in the calcined samples.

The proposed structure for the sulfated MCM-41 is shown in Scheme 2 [12]. Proposed structure for the sulfate containing MCM-41 material shows possible Brønsted acid sites (BA) and Lewis acid sites (LA).

In Scheme 2, it is shown that the sulfate group is covalently bonded to the silicon via oxygen atoms. The negative charge of the oxygen is neutralized by one proton forming BA. Due to



Scheme 2.

Table 2
Acidity of sulfated MCM-41

Sample code	Sulfate content (wt.%)	Acidity (mol/g)	
		PY	2,6-DMPY
MCM-41	0	283	220
2S/MCM-41	2	327	256
3S/MCM-41	3	355	292
4S/MCM-41	4	453	335
5S/MCM-41	5	346	283
6S/MCM-41	6	310	267
7S/MCM-41	7	307	258
8S/MCM-41	8	305	245

the inductive effect of the sulfate group, a strong LA site can be generated on its surface.

From the BET method the surface area of MCM-41 was found to be $1380\text{ m}^2/\text{g}$. It gradually decreased from 1380 to $980\text{ m}^2/\text{g}$ as the sulfate amount increased from 2 to 8 wt.%. This may be due to the blocking of pores of MCM-41 by sulfate. However the specific pore volume, average pore diameter and unit cell parameter remains practically the same (Table 1).

The total acid sites and Brønsted acid sites were measured by irreversible adsorption of pyridine (PY) and 2,6-dimethyl pyridine (2,6-DMPY), respectively. The data is shown in Table 2. Both the acid sites gradually increased with increase in sulfate content up to 4 wt.% and thereafter decreased.

The initial increase in surface acidity with increase in sulfate loading up to 4 wt.% may be due to sulfate monolayer formation. The decrease in surface acidity at high sulfate content is probably due to the formation of poly sulfate, which decreased the number of Brønsted acid sites and consequently that of total acid sites [15].

Table 1
Surface properties of sulfated MCM-41

Sample code	Sulfate (wt.%)	BET surface area ^a (m^2/g)	Wall thickness (Å)	Pore volume (cm^3/g)	Pore diameter (Å)	Unit cell parameter ^b (Å)
MCM-41	0	1380	24.1	1.28	37	46
2S/MCM-41	2	1285	23.6	1.26	39	45
3S/MCM-41	3	1227	22.5	1.23	40	44
4S/MCM-41	4	1154	23.3	1.19	41	45
5S/MCM-41	5	1093	24.2	1.17	42	44
6S/MCM-41	6	1021	23.3	1.18	46	42
7S/MCM-41	7	997	24.5	1.21	48	45
8S/MCM-41	8	980	24.3	1.2	48	43

^a Measured by nitrogen physisorption at liquid nitrogen temperature.

^b Unit cell parameter = $2/\sqrt{3} \times 100d$ (from XRD).

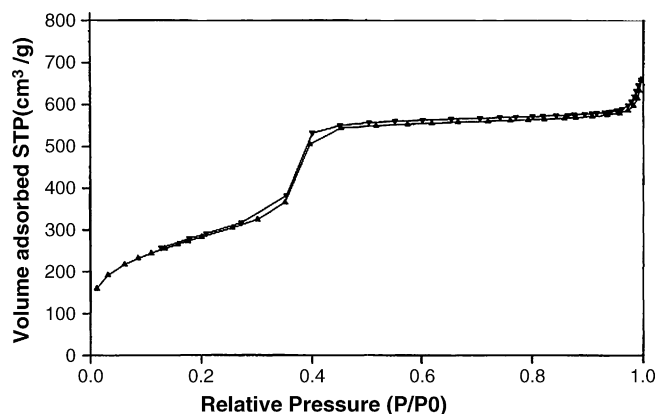


Fig. 3. N₂ adsorption–desorption isotherms of MCM-41 (▲, adsorption branch; ▼, desorption branch).

The adsorption and desorption isotherms of nitrogen are shown in Fig. 3. It showed that initially the adsorbed amount increased gradually with an increase in relative pressure by multilayer adsorption. Then, a sudden uptake of adsorbed amount was observed over a narrow range of relative pressure (P/P_0) between 0.25 and 0.35 is due to capillary condensation of nitrogen in the mesopores. The desorption branch of the isotherm coincides over the adsorption branch [16].

The thermo gravimetric curve of as-synthesized MCM-41 is shown in Fig. 4. The weight loss below 150 °C corresponds to the desorption of physisorbed water in the voids formed in the mesopores. Weight losses in the temperature range of 150–310 °C are due to the decomposition and removal of occluded organics [17].

The DTA curve is shown in Fig. 5. From the figure it is clear that there is almost no exothermal peak after 550 °C, which indicated the complete removal of surfactant.

3.1. Catalytic activity

The results of nitration of phenol using nitric acid over different wt.% of sulfated MCM-41 catalyst are given in Table 3. Among the catalysts studied, 4 wt.% S/MCM-41 showed highest conversion (93%) and selectivity (90%) for *ortho*-nitrophenol. The conversion as well as the selectivity to *ortho* isomer gradu-

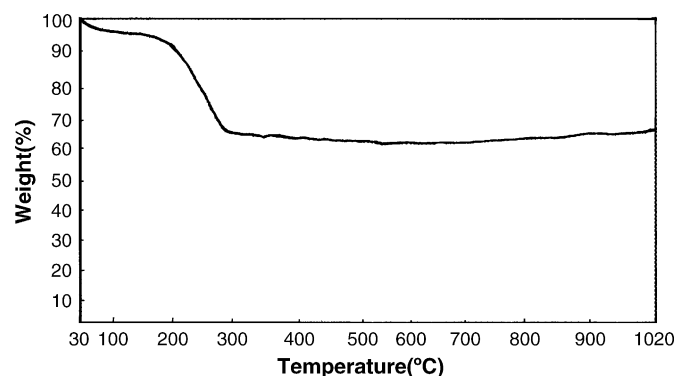


Fig. 4. Thermo gravimetric analysis curve of MCM-41.

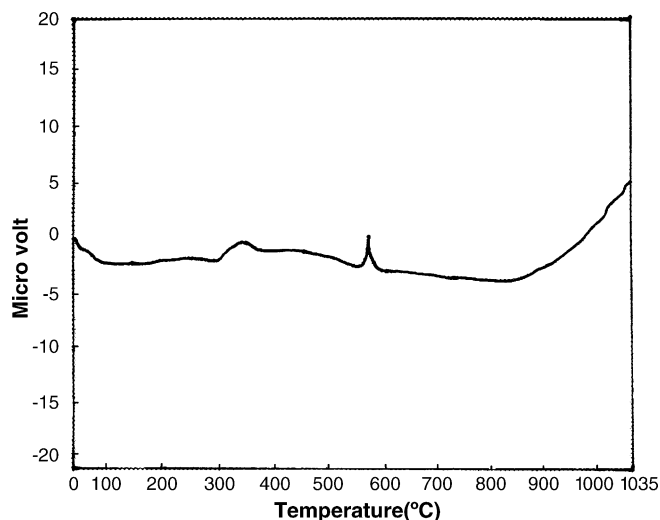


Fig. 5. Differential thermal analysis curve of MCM-41.

ally increases with increase in the sulfate amount up to 4 wt.% then after it decreases. The increase in activity as well as selectivity of the catalysts with the increase in sulfate amount might be due to an increase in the number of Brønsted acid sites. The decrease in conversion at high sulfate loading is probably due to formation of poly sulfate, which decreased the number of Brønsted acid sites.

When the reaction was carried out with MCM-41 (without sulfate) the conversion was only 31% with nearly equal *ortho* and *para* isomers, suggesting the influence of solid acid catalyst on the conversion and selectivity.

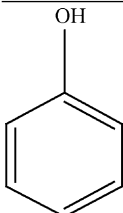
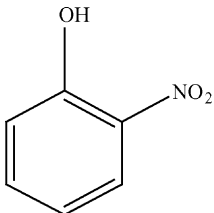
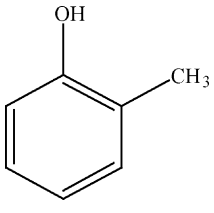
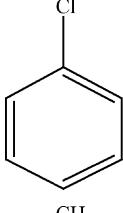
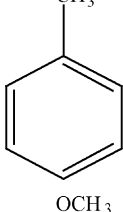
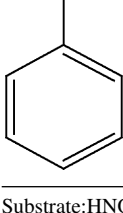
A number of different substrates were subjected to the nitration reaction and the results are summarized in Table 4. The results show that introduction of an electron withdrawing group (e.g. $-\text{NO}_2$ group) on phenol substantially decreases the percentage of conversion while an electron donating group (e.g. $-\text{CH}_3$ group) increases it. Activated substrates such as toluene and anisole gave 74% and 96% conversions, respectively. This is due to the ring activating nature of the substituents attached to the benzene ring. But under similar conditions chlorobenzene gave only 19% conversion due to the deactivating nature of chloride group.

Table 3
Effect of sulfated MCM-41 on nitration of phenol

Sample code	Conversion (%)	Selectivity (%)			O/P ratio
		oNP	pNP	BEZ	
MCM-41	31	52	48	–	1.08
2S/MCM-41	65	68	31	1	2.19
3S/MCM-41	71	82	16	2	5.10
4S/MCM-41	93	90	8	2	11.25
5S/MCM-41	86	75	23	2	3.26
6S/MCM-41	82	61	38	1	1.60
7S/MCM-41	75	58	40	2	1.45
8S/MCM-41	60	55	44	1	1.25

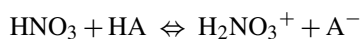
Phenol/HNO₃, 1; catalyst, 0.05 g; temperature, RT; HNO₃, 30%; solvent, DCE; reaction time, 2 h.

Table 4
Nitration of various substrates over sulfated MCM-41 catalyst

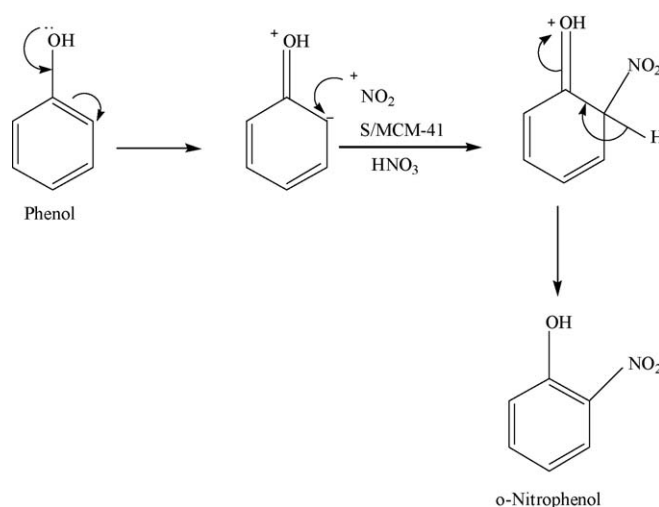
Substrate	Conversion (%)	Selectivity (%)	
		Ortho product	Para product
	93	90	8
	48	12	86
	96	11	88
	19	16	82
	74	60	39
	96	22	76

Substrate:HNO₃, 1:1; catalyst, 0.05 g; temperature, RT; HNO₃, 30%; solvent, DCE; reaction time, 2 h.

The mechanism that may be proposed for the reaction is given in Scheme 3:



Similarly when the attack of nitronium ion is at para position, *para*-nitrophenol is formed.



Scheme 3.

Here the reaction takes place between nitric acid and the Brønsted acid sites of the catalyst forming nitronium ion. Then electrophilic attack of nitronium ion on phenol takes place resulting in the formation of *ortho*- and *para*-nitrophenol. The variation of different reaction parameters was studied on 4S/MCM-41.

Fig. 6 explains the conversion of phenol with variation of molar ratio of phenol to nitric acid. Varying the molar ratio of phenol to nitric acid from 1 to 3, the percentage of conversion decreased but the selectivity towards *para*-nitrophenol increased. Similar results obtained by Degade et al. [13].

The influence of time on phenol nitration using 4S/MCM-41 is shown in Fig. 7. It was found that as the time increased from 0.5 to 2 h, the conversion of phenol to mono nitrophenol increased from 65% to 93% in 2 h then it remains constant, suggesting the influence of time on conversion. The selectivity towards *ortho*-nitrophenol does not affect significantly.

Fig. 8 shows the effect of nitric acid concentration on nitration of phenol over 4S/MCM-41. The phenol conversion increased with increase in nitric acid concentration up to 30% and then decreased with further rise in nitric acid concentration up to 70%. When nitric acid is diluted with water to 30%, the reaction medium is a three-phase system, i.e. solid acid catalyst, organic

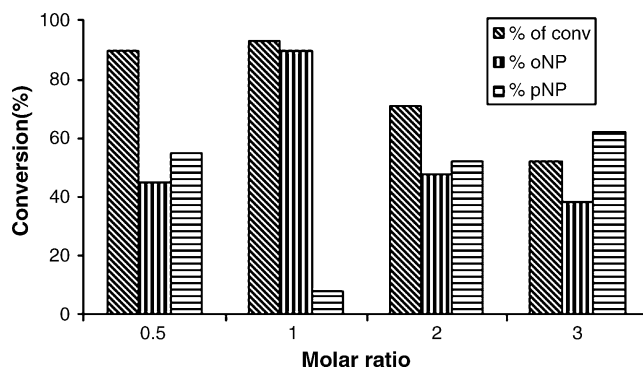


Fig. 6. Influence of phenol/nitric acid molar ratio on conversion of phenol. Catalyst, 0.05 g; temperature, RT; solvent, DCE; reaction time, 2 h; oNP, *ortho*-nitrophenol; pNP, *para*-nitrophenol.

Table 5
Effect of various catalysts on nitration of phenol

Catalyst	Conversion of phenol (%)	Selectivity				O/P ratio
		oNP	pNP	BEZ	tNP	
4S/MCM-41	93	90	8	2	–	11.25
H-ZSM-5	60	57	37	8	–	1.48
H-Y	60	60	30	10	–	2.0
Sulfated titania	85.6	92.4	3.9	–	1.4	23.6

tNP, 2,4,6-trinitrophenol.

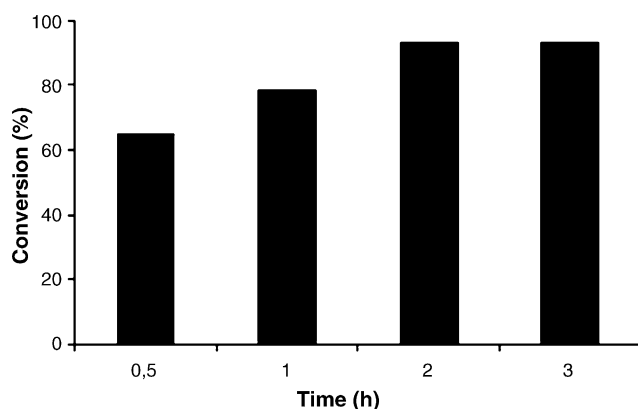


Fig. 7. Influence of time on conversion of phenol. Phenol/HNO₃, 1; catalyst, 0.05 g; temperature, RT; solvent, DCE.

solvent and aqueous phase. This triphasic system may be more active in nitration of phenol. At higher dilution (10–20%) of sulfuric acid the activity of HNO₃ is low leading to lower conversion suggesting 30% HNO₃ is suitable for nitration of phenol.

Formation of dinitrophenol was observed when the reaction was carried out using 70% nitric acid. Degade et al. [13] reported similar observation with higher concentration of nitric acid using modified zeolite as solid acid catalyst.

In similar reaction conditions, Degade et al. [13] reported 60% conversion using H-ZSM-5 and H-Y as solid acid catalysts. They found the selectivity ratio (oNP/pNP) is 1.48 and 2.0 for H-ZSM-5 and H-Y, respectively. Similarly, the results obtained by Sunajadevi and Sugunan [18] using sulfated titania as catalyst have been compared with the present work (Table 5).

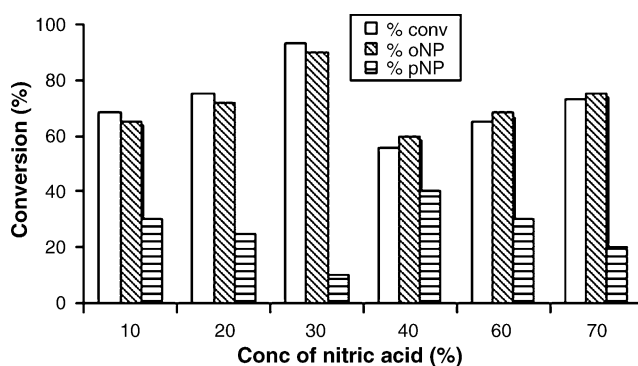


Fig. 8. Influence of concentration of nitric acid on conversion of phenol. Phenol/HNO₃, 1; catalyst, 0.05 g; temperature, RT; solvent, DCE; reaction time, 2 h; oNP, *ortho*-nitrophenol; pNP, *para*-nitrophenol.

3.2. Reusability of the catalyst

The reusability of the catalyst was studied by using 4S/MCM-41 in recycling experiments. In order to regenerate the catalyst, after 2 h of reaction, it was separated by filtration, washed several times with conductivity water, dried and calcined at 550 °C and used in the nitration reaction with a fresh reaction mixture. In the regenerated sample after three cycles, the yield decreased by 5%.

4. Conclusions

- (1) From the fore going discussion it is concluded that, the nanostructured MCM-41, synthesized by sol–gel method presents good stability according to various physico-chemical characterizations.
- (2) Modification of MCM-41 with H₂SO₄ generated active Brønsted and Lewis acid sites in MCM-41. The 4 wt.% sulfated MCM-41 showed the maximum acidity.
- (3) From the BET surface area and XRD study, the samples are found to be mesoporous. The BET surface area gradually decreased with increase in sulfate loading, where as the pore volume and pore diameter remain practically the same.
- (4) The 4S/MCM-41 showed maximum conversion (93%) and selectivity (90%) towards nitration of phenol.

Acknowledgments

The authors are thankful to Prof. B.K. Mishra, Director, RRL for his keen interest, encouragement and kind permission to publish this work. The authors are thankful to RSIC, IIT Mumbai, for their help in FT-IR and TG–DTA analysis. Financial assistance to one of the authors, Mrs D. Rath by CSIR is gratefully acknowledged.

References

- [1] C.T. Kresge, M.E. Leonowicz, W.J. Roth, J.C. Vartuli, US Patent 5098684 (1992).
- [2] C.T. Kresge, M.E. Leonowicz, W.J. Roth, J.C. Vartuli, J.S. Beck, Nature 352 (1992) 710.
- [3] G. Buchel, K.K. Unger, A. Matsumoto, K. Tatsumi, Adv. Mat. 10 (1998) 1036.
- [4] J.S. Beck, J.C. Vartuli, W.J. Roth, M.E. Leonowicz, C.T. Kresge, K.D. Schmitt, C.T.W. Chu, D.H. Olson, E.E. Sheppard, S.B. McCullen, J.B. Higgins, J.L. Schlenker, J. Am. Chem. Soc. 114 (1992) 10834.
- [5] G.D. Ganapati, J.J. Nair, Micropor. Mesopor. Mater. 33 (1999) 1.

- [6] V.N. Romnikov, V.B. Fenelonov, B.A. Paukshtis, A.Y. Derevyanku, V.I. Zaikovskii, *Micropor. Mesopor. Mater.* 21 (1998) 411.
- [7] A. Galarneau, D. Desplantie-Giscard, F. Di Renzo, F. Fajula, *Catal. Today* 68 (2001) 191.
- [8] V.Y. Gusev, X.B. Feng, Z. Bu, G.L. Haller, J.A. Obrien, *J. Phys. Chem.* 100 (1996) 1985.
- [9] A. Corma, V. Fornes, M.T. Navarro, J. Perez-Pariente, *J. Catal.* 148 (1994) 569.
- [10] C.T. Kresge, M.E. Leonowicz, W.J. Roth, J.C. Vartuli, J.S. Beck, *Nature* 359 (1992) 710.
- [11] P. Trens, M.L. Russell, L. Spjuth, M.J. Hudson, J. Liljenzin, *Mater. Interf.* 41 (2002) 5220.
- [12] J.M.F.B. Aquino, C.D.R. Souza, A.S. Araaju, *Int. J. Inorg. Mater.* 3 (2001) 467.
- [13] S.P. Degade, V.S. Kadam, M.K. Dongare, *Catal. Commun.* 3 (2002) 67.
- [14] J.S. Beck, J.C. Vartuli, W.J. Roth, M.E. Leonowicz, C.T. Kresge, K.D. Schmitt, C.T.W. Chu, D.H. Olson, E.W. Sheppard, S.B. McCullen, Y.B. Higgins, I.L. Schlenker, *J. Am. Chem. Soc.* 102 (1992) 1.
- [15] J. Navarrette, T. Lopez, R. Gomez, *Langmuir* 12 (1996) 4385.
- [16] M. Grun, K.K. Unger, A. Matsumoto, K. Tsutsumi, *Micropor. Mesopor. Mater.* 27 (1999) 207.
- [17] M. Selvaraj, K. Lee, K.S. Yoo, T.G. Lee, *Micropor. Mesopor. Mater.* 81 (2005) 343.
- [18] K.R. Sunajadevi, S. Sugunan, *Catal. Commun.* 6 (2005) 611.